14

# Some Complexity Studies of Electroseismic Signals from Mexican Subduction Zone

L. Guzmán-Vargas[1], R. Hernández-Pérez[1], F. Angulo-Brown[1] and A. Ramírez-Rojas[2]
[1]*Instituto Politécnico Nacional*
[2]*Universidad Autónoma Metropolitana - Azcapotzalco*
*México*

## 1. Introduction

The analysis of complex signals associated to geoelectric activity is important not only for earthquake prognosis but also for understanding non linear processes related to earthquake preparation. Previous studies have reported alterations, such as the emergence of correlated dynamics in geoelectric potentials prior to an important earthquake (EQ). One important feature of geoelectric signals is the absence of regularity patterns with fluctuations apparently influenced by noise. In past decades, earthquake prediction methods have attracted the attention of researchers from different areas of science. The search for effective seismic precursors has not been successful. However, despite some pessimism, in many seismically actives zones around the world there exist research programs for the study of possible precursory phenomena of earthquakes(Cicerone et al., 2009; Hayakawa, 1999; Hayakawa & Molchanov, 2002; Lomnitz, 1990; Telesca & M., 2005; Uyeda et al., 2000; Varotsos et al., 2003a;b;c; 2004; 2005). In particular, one of the techniques used in the search of earthquake precursors since more than three decades ago consists in monitoring the so-called electric self-potential field. The main motivation to explore this kind of signals is that it is expected that before the occurrence of an earthquake (Varotsos, 2005), the stress (pressure) gradually varies in the focal area, which affects various physical properties, for example the static dielectric constant (Varotsos, 1980; 1978). In addition, this stress variation may change the relaxation time for the orientation of the electric dipoles formed due to lattice defects (Lazaridou et al., 1985). It may happen that, when the stress (pressure) reaches a critical value (Varotsos & Alexopoulos, 1984b), these electric dipoles exhibit a cooperative orientation (collective organization), thus leading to emission of transient electric signals termed Seismic Electric Signals, SES (Uyeda et al., 2000; Varotsos & Alexopoulos, 1984a). This generation mechanism of signal emission is named pressure stimulated polarization currents (PSPC) (Varotsos & Alexopoulos, 1986). It is expected that precursory electric signals associated with large earthquakes should exhibit anomalous changes and, in some cases, fractal complex organization (Varotsos, 2005; Varotsos et al., 2003c; 2004). Additionally, several other physical mechanisms have been proposed as possible causes of electromagnetic (EM) precursory signals before EQ's, such as electrokinetic effects (EK) (Haartsen & Pride, 1997; Ishido & Mizutani, 1981; Mizutani et al., 1976), piezoelectric effects (PE) (Gershenzon et al.,

1993) and electromagnetic induction effects (Gershenzon et al., 1993; Honkura et al., 2000; Iyemori et al., 1996; Matsushima et al., 2002). A very recent review about PSPC, EK, PE and other possible generation mechanisms of signal emissions can be seen in Uyeda et al. (Uyeda et al., 2008). We have measured the ground electrical potential (the self-potential) in several sites along the Mexican coast, near the Middle American trench, which is the border between the Cocos and the American tectonic plates. In some previous articles we have reported more detailed descriptions of that region and some studies of possible precursory electric phenomena associated to several earthquakes of magnitude larger than six (Flores-Márquez et al., 2007; Muñoz Diosdado et al., 2004; Ramírez-Rojas et al., 2007). Recent studies focused on fractal and non linear properties of physical and biological times series have revealed that this organization is strongly related to a complex interaction of multiple components and mechanism across multiple scales. In particular, published studies about the complexity of ground electric self-potential behavior have pointed out that changes inthe fractal organization have been observed in a period prior to an important earthquake. However, a clear evidence with statistical support about the mechanisms involved in these changes, has not been presented, although some important suggestions and discussions have been proposed to address this problem (Gotoh et al., 2003; 2004; Ida et al., 2005; 2006; Smirnova et al., 2004; Telesca & Lapenna, 2006; Varotsos et al., 2008). One important feature of geoelectric signals is the absence of regularity patterns. These fluctuations are embedded into noise activity produced by the combined contribution of many high-dimensional processes, which due to the central-limit theorem, are Gaussian-distributed. The direct application to this kind of signals of nonlinear methods such as power spectrum, detrended fluctuation analysis (DFA) and fractal dimension method reveals that different correlation levels are present in the vicinity of a main shock. Very often the double log plot of scaling exponents obtained from the aforementioned methods present a crossover behavior between different scales. On the other hand, a long term relaxation-EQ-preparation-main shock-relaxation process has been reported before some large EQ's (Varotsos, 2005). From this point of view, one could expect that a relaxed surface layer of earth's crust corresponds to white noise in geoelectric signals and the EQ-preparation process corresponds to a background white noise mixed with a kind of correlated geoelectric signals expressed through a crossover behavior. However, this idea must be taken as a speculative hypothesis which requires a more profound attention. Thus, in this context is very important to incorporate a variety of methods to statistically distinguish and evaluate these complex dynamics.

In this chapter, we report some complexity studies of geoelectric signals during a two year period from Jun 1st. 1994 to May 31st 1996 in two sites (Acapulco and Coyuca stations) located in southern Mexico. In particular, our study is related to an $Ms = 7.4$ earthquake occurred on September 14, 1995 with epicentral distance of 110 km from Acapulco and 200 km from Coyuca, respectively. Previous studies have reported changes in the correlation dynamics observed prior to this earthquake (Guzmán-Vargas et al., 2008; Ramírez-Rojas et al., 2008; 2007; 2004; Telesca et al., 2009). However, the possible existence of seismic precursors associated with this event has not been deeply explored. Here, we perform a systematic study of DFA exponents and sample entropy to evaluate the level of irregularity and correlations of geoelectric time series. We observe important changes in the entropy a few months before the occurrence of the earthquake mentioned above. On the other hand, we use a procedure to statistically estimate two DFA-scaling exponents and the crossover

scale which are representative of changes in the underlying dynamics prior to the main shock. Moreover, we perform a pattern synchrony analysis based on the computation of the cross-sample entropy between the geoelectric signals from two channels, which represents a modern approach to the study of geoelectric signals. The chapter is organized as follows. In Sec. 2, a brief description of the entropy and the detrended fluctuation analysis methods are presented. We also describe the geolectric time series. In Sec. 3, we present the results and discussions. Finally, some concludings remarks are presented.

## 2. Methods and data

### 2.1 Entropy methods

The entropy of a single discrete random variable $X$ is a measure of its uncertainty. In the case of a stochastic process, the mean rate of creation of information is measured by the Kolmogorov-Sinai (KS) entropy (Eckmann & Ruelle, 1985). However, the KS entropy is not applicable to finite length real world series because only entropies of finite order can be computed numerically and KS is underestimated as the order becomes large. An alternative procedure to estimate the entropy of a signal was given by Grassberger et al. (Grassberger & Procaccia, 1983). They proposed the $K_2$ entropy to characterize chaotic systems which is a lower bound of the $KS$ entropy. Later, based on $K_2$ definition, Pincus introduced the *Approximate Entropy* ($ApEn$) to quantify the regularity in time-series (Pincus, 1991; 1995). Briefly, $ApEn$ is constructed as follows: given a time series $X_i = x_1, ..., x_N$ of length $N$. First, $m$-length vectors are considered: $u_m(i) = x_i, x_{i+1}, ..., x_{i+m-1}$. Let $n_{im}(r)$ represent the number of vectors $u_m(j)$ within $r$ of $u_m(i)$. $C_m^i(r) = n_{im}(r)/(N-m+1)$ is the probability that any vector $u_m(j)$ is within $r$ of $u_m(i)$. Next, the average of $C_m^i$ is constructed as $\Phi^m(r) = 1/(N-m+1)\sum_{i=1}^{N-m+1} \ln C_i^m(r)$. Finally, $ApEn$ is defined as $ApEn(m,r) = lim_{N\to\infty}\left[\Phi^m(r) - \Phi^{m+1}(r)\right]$: which, for finite $N$, it is estimated by the statistics $ApEn(m,r,N) = \Phi^m(r) - \Phi^{m+1}(r)$. In words, the statistics $ApEn(m,r,N)$ is approximately equal to the negative average natural logarithm of the conditional probability that two sequences that are similar for $m$ points remain similar at the next point, within a tolerance $r$ (Richman & Moorman, 2000). It is obtained that a low value of $ApEn$ reflects a high degree of regularity. Even though the implementation and interpretation of $ApEn$ is useful to distinguish correlated stochastic processes and composite deterministic/stochastic models (Pincus, 1995), it has been found there is a bias in $ApEn$ because the algorithm counts each sequence as matching itself (Richman & Moorman, 2000). The presence of this bias causes $ApEn$ to lack two important expected properties: (a) $ApEn$ is heavily dependent on the time-series length and is uniformly lower than expected for short series and, (b) it lacks relative consistency in the sense that if the value of $ApEn$ for a time-series is higher than that of another, it does not remain so if the test conditions change (Pincus, 1995). Therefore, the development of an alternative method was desirable to overcome the limitations of $ApEn$. Based on $K_2$ and $ApEn$ methods, Richman and Moorman (Richman & Moorman, 2000) introduced the so-called Sample Entropy ($S_E$), to reduce the bias in $ApEn$. One of the advantages of $S_E$ is that does not count self-matches and is not based on a template-wise approach (Richman & Moorman, 2000). $S_E(m,r,N)$ is precisely defined as

$$S_E(m,r,N) = -\ln \frac{U^{m+1}}{U^m}, \tag{1}$$

that is, the negative natural logarithm of the conditional probability ($U$) that two sequences similar for $m$ points remain similar at the next point, within tolerance $r$, without counting the self-matches. $S_E$ results to be more robust than $ApEn$ statistics when applied to short time series from different stochastic processes over a wide range of operating conditions. For instance, a lower value of $S_E$ indicates a more regular behavior of a time-series whereas high values are assigned to more irregular, less predictable, time series (Costa et al., 2005). It applies to realworld time series and, therefore, has been widely used in physiology and medicine (Costa et al., 2005).

### 2.2 Cross sample entropy

Entropy can also be calculated between two signals, and this mutual entropy characterizes the probability of finding similar patterns within the signals. Therefore, the cross-entropy technique was introduced to measure the degree of asynchrony or dissimilarity of two time series (Pincus, 1995; Pincus & Singer, 1996).

When calculating the cross-entropies, the patterns that are compared are taken in pairs from the two different time series $\{u(i)\}$ and $\{v(i)\}$, $i = 1, \ldots, N$. The vectors are constructed as follows:

$$\mathbf{x}_m(i) = [u(i), u(i+1), u(i+2), \ldots, u(i+m-1)],$$
$$\mathbf{y}_m(i) = [v(i), v(i+1), v(i+2), \ldots, v(i+m-1)],$$

with the vector distance defined as

$$d[\mathbf{x}_m(i), \mathbf{y}_m(j)] = max\{|u(i+k) - v(j+k)| : 0 \leq k \leq m-1\}.$$

With this definition of distance, the $S_E$ algorithm can be applied to compare sequences from the *template* series to those of the *target* series to obtain the Cross Sample Entropy ($C_E$). It is usual that the two time series are first normalized by subtracting the mean value from each data series and then dividing it by the standard deviation. This normalization is valid since the main interest is to compare patterns.

It is quite possible that no vectors in the target series can be found to be within the distance $r$ to the template vector and then the value of $C_E$ is not defined. One important property of $C_E$ is that its value is independent of which signal is taken as a template. In particular, the Cross Sample Entropy is used to define the *pattern synchrony* between two signals, where synchrony refers to pattern similarity, not synchrony in time, wherein patterns in one series appear (within a certain tolerance) in the other series. Moreover, $C_E$ assigns a positive number to the similarity (synchronicity) of patterns in the two series, with larger values corresponding to greater common features in the pattern architecture and smaller values corresponding to large differences in the pattern architecture of the signals (Veldhuis et al., 1999). When no matches are found, a fixed negative value is assigned to $C_E$ to allow a better displaying of the results.

The conceptual difference between pattern synchrony, as measured by the $C_E$, and correlations, as measured by the cross-correlation function, can be expressed as follows: let us suppose that we have two time series $\{x(k)\}$ and $\{y(k)\}$. The $C_E$ deals with patterns: a sequence of data points of a certain length $m$ is taken from the template time-series $\{x(k)\}$

and this pattern is searched for in the target time-series $\{y(k)\}$ within a tolerance $r$. However, the $C_E$ does not collect the time-stamp of the matching sequence in the time series $\{y(k)\}$, but counts the number of sequence matches of lengths $m$ and $m+1$. On the other hand, the objective of the cross-correlation function is to find the time lag $\tau$ for which the whole time series $\{x(k)\}$ resembles $\{y(k)\}$, but the time series are not decomposed in sequences of points. Therefore, the $C_E$ analysis is complementary to the cross-correlation and spectral analysis since it operates on different features of the signals (see the *Appendix* of Ref. Pincus & Singer (1996)).

### 2.3 Multiscale entropy analysis

Recently, Costa et al. (Costa et al., 2002) introduced the multiscale entropy analysis (MSE) to evaluate the relative complexity of normalized time series across multiple scales. This procedure was proposed to give an explanation to the fact that, in the context of biological signals, single-scale entropy methods ($S_E$ and $ApEn$) assign higher values to random sequences from certain pathological conditions whereas an intermediate value is assigned to signals from healthy systems (Costa et al., 2002). It has been argued that these results may lead to erroneous conclusions about the level of complexity displayed by these systems (Costa et al., 2005). The MSE methodology shows that long-range correlated noises as the output of healthy systems are more complex than uncorrelated signals from some pathological conditions. Briefly, the the MSE method consists of: given a time series $X_i = x_1, ..., x_N$, a coarse-grained procedure is applied (Costa et al., 2005). A scale factor $\tau$ is introduced to perform a moving average given by $y_j = 1/\tau \sum_{i=(j-1)\tau+1}^{j\tau} x_i$, with $1 \leq j \leq N/\tau$. Note that the length of the coarse-grained time series is given by $N/\tau$, that is, for scale one the original time series is obtained. To complete the MSE procedure the $S_E$ algorithm is applied to the coarse-grained time series for each scale. Finally, the entropy value is plotted against the scale factor. Typically, under MSE analysis, the entropy values for a random noise monotonically decreases whereas for long-range correlated noise ($1/f$-noise) the entropy remains constant for several scales, indicating that $1/f$-noise is structurally more complex than uncorrelated signals (Costa et al., 2005).

### 2.4 DFA method

The power spectrum is the typical method to detect correlations in a time series. For example, consider a stationary stochastic process with autocorrelation function which follows a power law

$$C(s) \sim s^{-\gamma}, \tag{2}$$

where $s$ is the lag and $\gamma$ is the correlation exponent, $0 < \gamma < 1$. The presence of long-term correlations is related to the fact that the mean correlation time diverges for infinite time series. According to the Wiener-Khintchine theorem, the power spectrum is the Fourier transform of the autocorrelation function $C(s)$ and, for the case described in Eq. 2, we have the scaling relation,

$$S(f) \sim f^{-\beta}, \tag{3}$$

where $\beta$ is called the spectral exponent and is related to the correlation exponent by $\gamma = 1 - \beta$. When the power spectrum method is used to estimate the presence of correlations

in real nonstationary time series, as in the case of heartbeat interval signals, it may lead to unreliable results. In past decades, alternative methods have been proposed to the assessment of correlations for stationary and nonstationary time series. A method which is very appropriated to the assessment of correlations in stationary and nonstationary time series is the detrended fluctuation analysis (DFA). This method was introduced to quantify long-range correlations in the heartbeat interval time series and DNA sequences (Peng et al., 1995a;b). The DFA is briefly described as follows: First, we integrate the original time series to get, $y(k) = \sum_{i=1}^{k} [x(i) - x_{ave}]$, the resulting series is divided into boxes of size $n$. For each box, a straight line is fitted to the points, $y_n(k)$. Next, the line points are subtracted from the integrated series, $y(k)$, in each box. The root mean square fluctuation of the integrated and detrended series is calculated by means of

$$F(n) = \sqrt{\frac{1}{N}\sum_{k=1}^{N}[y(k) - y_n(k)]^2}, \tag{4}$$

this process is taken over several scales (box sizes) to obtain a power law behavior $F(n) \sim n^{\alpha}$, with $\alpha$ an exponent, which reflects self-similar and correlation properties of the signal. The scaling exponent $\alpha$ is related to the spectral exponent $\beta$ by means of $\alpha = (\beta + 1)/2$ (Peng et al., 1995a). It is known that $\alpha = 0.5$ is associated to white noise (non correlated signal), $\alpha = 1$ corresponds to $1/f$ noise and $\alpha = 1.5$ represents a Brownian motion. This exponent is also related to the autocorrelation function exponent by $\alpha = 1 - \gamma/2$ where the autocorrelation function is $C(\tau) \propto \tau^{-\gamma}$ with $0 < \gamma < 1$ (Makse et al., 1996).

### 2.5 Data

The time series considered in this study were collected during a two year period, from June 1994 to May 1996, in two electroseismical stations located at Acapulco (16.85 N, 99.9 W) and Coyuca (18.35 N, 100.7 W), both located in the South Pacific coast in Mexico (Ramírez-Rojas et al., 2004). The electrical signals consist of the electric self-potential fluctuations $V$ between two electrodes buried 2 m into the ground and separated by a distance of 50 m. Each pair of electrodes was oriented in one direction: North-South and East-West, as it is indicated by VAN methodology (Varotsos & Alexopoulos, 1984a;b). Two time series were simultaneously recorded at each electroseismic station (N-S and E-W channels). Due to technical adjustments, two different sampling rates were used in different time intervals along the mentioned period, $t = 4$ s in Coyuca and $t = 2$ s in Acapulco (Yépez et al., 1995). In Figure 1 representative time series of potential differences for one year period (Jan. 1st. to Dec. 31st. 1995) in Acapulco station are presented. During the period of study, two EQs with $M > 6$ occurred with epicenters within 250 km of the two monitoring stations. The first EQ occurred on September 14, 1995 with $M = 7.4$ and epicenter with coordinates (16.31 N, 98.88 W), with focal depth of 22 Km; the hypocenter was at $d = 112$ km from Acapulco and $d = 146.6$ km from Coyuca. The second EQ occurred on February 24, 1996 with $M = 7.0$ and epicenter with coordinates (15.8 N, 98.25 W), with focal depth of 3 Km; and hypocenter at $d = 220.02$ km from Acapulco and $d = 250.01$ km from Coyuca. As can be seen from Figure 2, the two earthquakes had epicenters located closer to the Acapulco station. The analyzed noisy time series were not preprocessed and non significant nonstationary features affecting the correlation properties

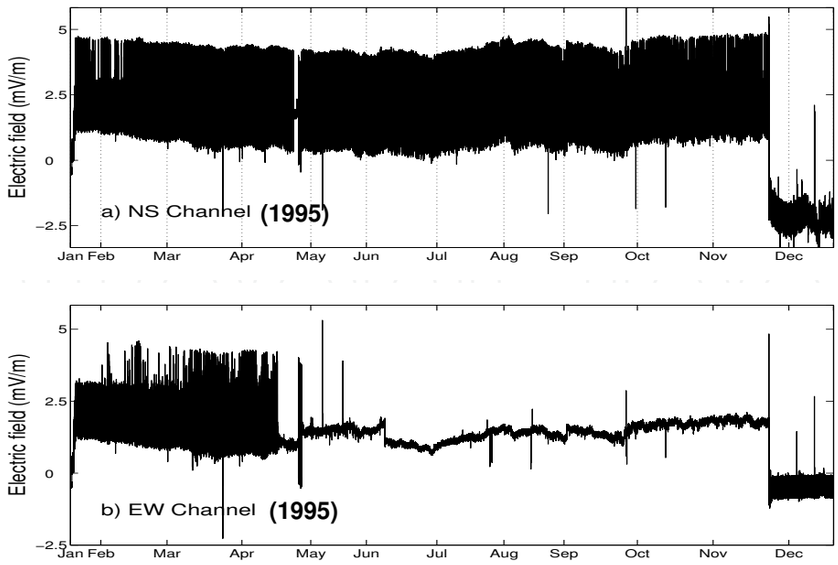


Fig. 1. Representative geoelectric time series from Acapulco station for one year period (Jan. 1st to Dec. 31st., 1995). **(a)** N-S channel and **(b)** E-W channel.

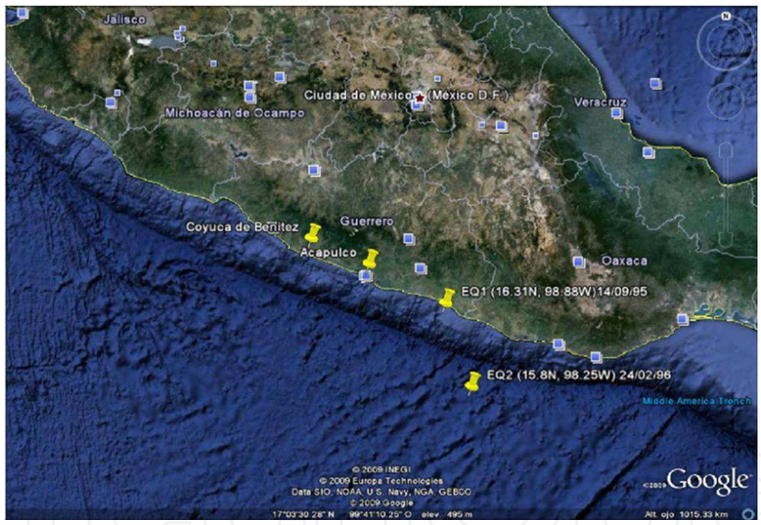


Fig. 2. Location of the monitoring stations and the epicenters of the earthquakes occurred during the studied time period.

of a signal mentioned by Chen et al. (Chen et al., 2002), were present in a remarkable way in our data. When comparing these two signals, different kind of fluctuations can be identified. An important question here is to evaluate the level of irregularity across multiple scales and its relation with the presence of long range correlations. We evaluate the changes in the variability by means of $S_E$, which estimates the amount of new information arriving at any time, the cross sample entropy and the presence of correlations by using the DFA method.

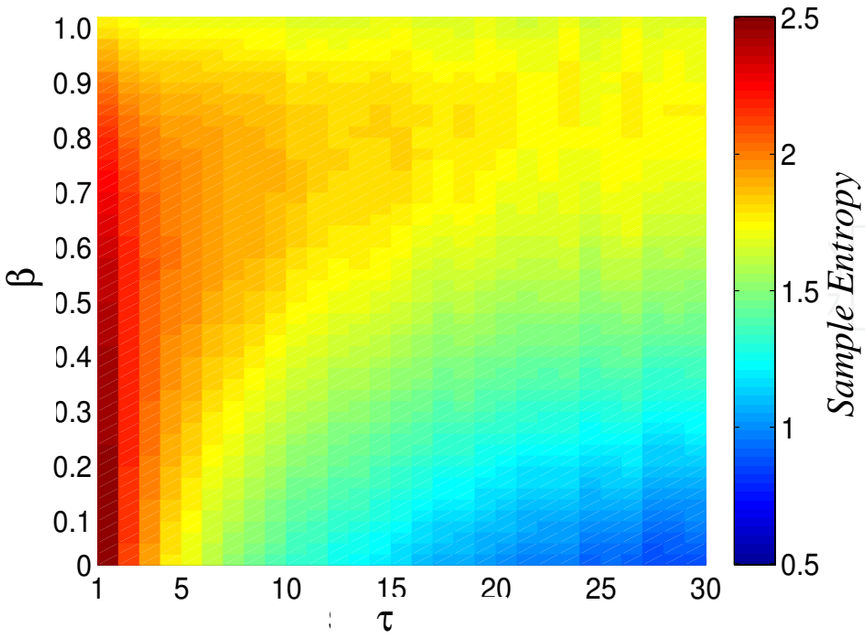


Fig. 3. Plot of MSE analysis for $1/f^{\beta}$-noises with $0 \leq \beta \leq 1$, that is, for noises with power-law correlations. We used the Fourier filtering method to generate time series of 32000 points. In this plot, each point represents the average of 10 independent realizations. The value of $S_E$ is given according to the color panel. Note that as the spectral exponent increases the entropy value remains high even for large time scales .

## 3. Results and discussion

### 3.1 MSE results

First, in order to get a better estimation of entropy values for Gaussian noises with power law correlations, we performed simulations of noises with power spectrum of the form $1/f^{\beta}$ with $0 \leq \beta \leq 1$. We generated time series with 32000 points by means of the Fourier filtering method (Makse et al., 1996). We applied the MSE analysis to the generated data for several values of $\beta$ in the interval $0 \leq \beta \leq 1$ and a range of time scales. In Fig. 3, the results for entropy are presented according to the color panel. Notice that for $\beta = 0$ and $\beta = 1$, the main results described in (Costa et al., 2002) are recovered. We observe that as the spectral exponent $\beta$ increases , that is, as long-range correlations are present, $S_E$ decreases moderately but at the same time remains constant for several time scales. This behavior indicates that, in the context of simulated signals, the amount of new information arriving at any time is "regulated" by the presence of correlations.

In order to apply the MSE procedure to the geoelectric time series we considered non overlapped time windows of 5,400 data points each, corresponding approximately to 3 hours of records Guzmán-Vargas et al. (2009). First, the data points of the original signal are divided by its standard deviation and $S_E$ is calculated for each time scale according to the MSE method. We repeated the MSE procedure for the corresponding shuffled version of each window. In all the cases presented here, we used the following values for parameters $r$ and

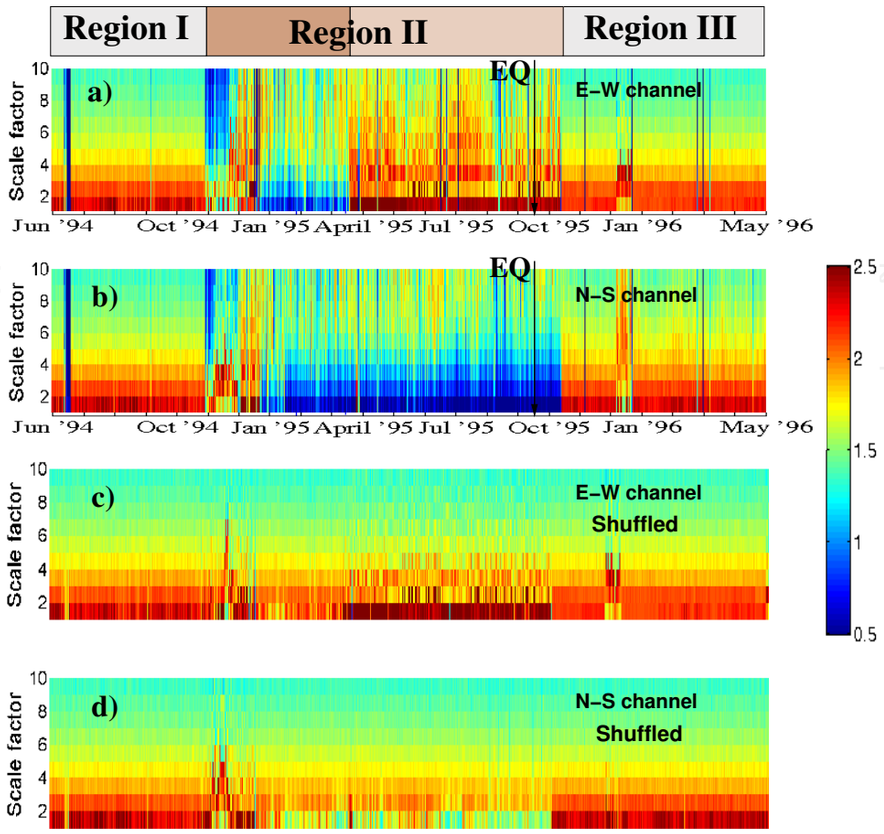


Fig. 4. MSE analysis of geoelectrical time series from Acapulco station. **(a)** MSE results for E-W channel, three main regions can be identified according to the changes of $S_E$ for different scale factors. Note that Region II is mostly characterized by a high entropy value even for large time scales. **(b)** Entropy results for N-S channel. In this case, Region I and III also display white noise profile whereas Region II shows high regularity for short scales. **(c)**, **(d)** As in **(a)** and **(b)** but for randomized data. Note that in these shuffled cases the data display mostly white noise profile (Guzmán-Vargas et al., 2009).

$m$: $r = 0.15$ and $m = 2$. In Fig. 4, the results of $S_E$ for both channels of Acapulco station are presented. The color panel represents the values of $S_E$ in the interval 0.5 to 2.5.

For the period from June 1994 to October 1994 we define Region I and we observe that during this period and in both channels, $S_E$ shows a high value for scale 1 and rapidly decreases as the scale factor increases as it occurs with white noise dynamics (Figs. 4(a) and 4(b)). We also identify region III from November 1995 to May 1996 where entropy values show a similar profile as in region I, that is, mostly white noise dynamics. For the period from November 1994 to October 1995, we define region II which is characterized by a complex behavior. For E-W channel, we observe that for a short interval at the beginning of this period, $S_E$ shows a low value for scale one and a small increment for large time scales is observed, followed by a new short period with complex behavior. After this transient behavior, the entropy is small for short scales, that is, a high regularity in the original data is observed . Interestingly, for the period comprising April 1995 to October 1995, the entropy profile reveals that $S_E$ remains

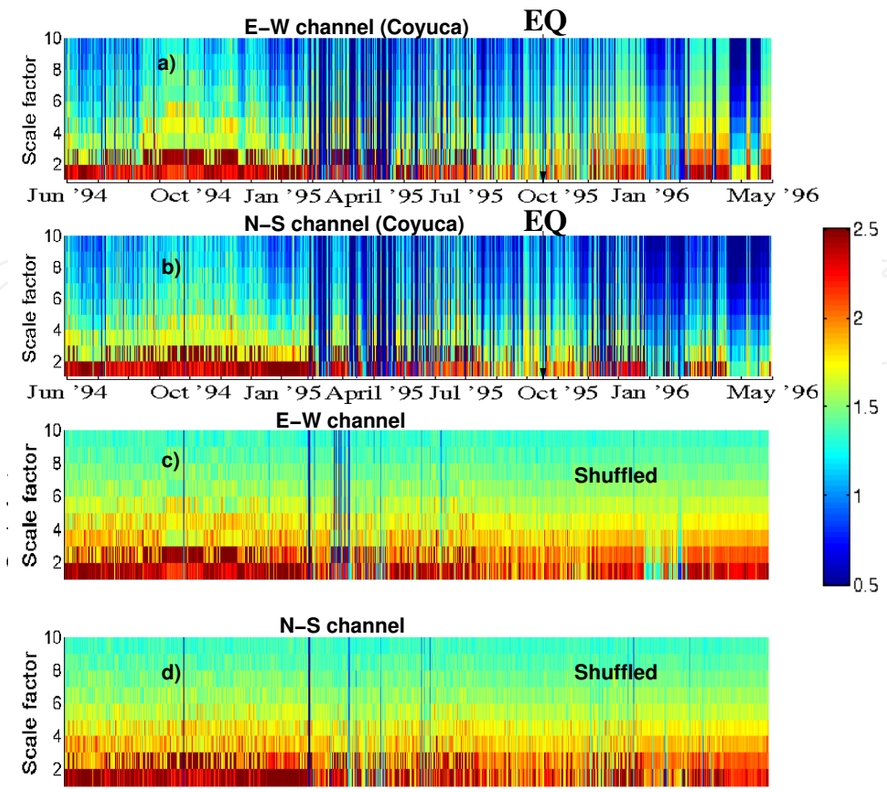


Fig. 5. MSE analysis of geoelectric time series from Coyuca station. **(a)** MSE results for E-W channel, we observe that entropy value is high for short scales and rapidly decreases such that for scales larger than $\tau = 6$ it shows high regularity, except for short periods with a low entropy at short scales. **(b)** Entropy results for N-S channel. **(c)**, **(d)** As in **(a)** and **(b)** but for randomized data. Note that in these cases the data display mostly white noise profile (Guzmán-Vargas et al., 2009)

high even for scale $\tau = 5$, indicating a presence of complex dynamics probably related to the presence of long range correlations (Fig. 4(a)).

For N-S channel (Fig. 4(b)), the entropy is small for scale one and shows a small increment as the scale factor increases, that is, more regularity in the fluctuations is present in the original time series. This behavior is observed for almost the whole period in region II, except for a short interval at the beginning where a transient very similar to the one identified in E-W channel is observed.

In Figs. 4(c) and 4(d) results for the corresponding shuffled versions are presented. For E-W data, we observe that for almost the whole two year period a pattern similar to white noise is present, except for a high value, corresponding to scale one, which is identified in the period of complex dynamics. For N-S channel, the entropy shows a profile similar to white noise. For Coyuca Station and for both channels, we observe that $S_E$-values are high for short scales indicating a high variability in the signals (see Figs. 5(a) and 5(b)). Another important features observed in both channels are the presence of multiple short periods with a

low entropy value across multiple scales and that entropy values rapidly decrease as the scale factor increases, indicating more regularity for large scales. When these results are compared to their corresponding surrogate sequences, the entropy profile is similar to white noise and the short periods with low entropy values are changed to uncorrelated dynamics (see Figs. 5(c) and 5(d)).

### 3.2 DFA results

To obtain further insights in the evaluation of the complex dynamics observed in some periods of the records and its relation with the presence of correlations, we apply the DFA method (Peng et al., 1995b). The DFA is applied to segments of the same length as in the case of entropy calculations (Guzmán-Vargas et al., 2009) . Representative cases of $F(n)$ vs. $n$ for some periods during 1995 (from Region II defined in Fig. 4(a)) are shown in Fig. 6. As we can see in these plots, two different scaling exponents can be defined to describe correlations. To get a better estimation of $\alpha$-values and the crossover point, we consider the following procedure: given the fluctuation values $F(n)$, a sliding pointer is considered to perform linear regression fits to the values on the left and to the elements on the right. At each position of the pointer, we calculate the errors in the fits ($e_l$ and $e_r$) and we monitored the total error defined by $e_t = e_l + e_r$. We define two stable exponents when $e_t$ reaches its minimum value and the position of the crossover point is within the interval $6 \leq n \leq 500$. The results of DFA exponents for two regimes (separated by the crossover point $n_\times$) from Acapulco and Coyuca are presented in Figs. 7 and 8.

For both channels in Acapulco station, as it occurred in MSE analysis, we identify three different regions which are characterized by different correlation dynamics. For region I, we see that $\alpha_1$ and $\alpha_2$ are quite similar each other with values around 0.5 which indicates a white noise behavior (see Fig. 7(a),(b)). For region III, defined from November 1995 to May 1996, we observe that the signals also display mostly white noise dynamics. Interestingly, for region II, that is, for a period comprising November 1994 to October 1995, the dynamics can be described by two values distinctly different, both of them higher than 0.5 and close to 1, indicating long-term correlations. A more detailed observation of the scaling exponents within this region in E-W channel (Fig. 7(a)) reveals that, from November 1994 to March 1995, $\alpha_1$ is close to the Brownian motion value ($\alpha_{BM} = 1.5$) whereas $\alpha_2$ oscillates and stabilizes around the white noise value. In the immediate period from April until October 1995, both scaling exponents are close to 1, indicating the presence of power-law correlations. For N-S channel, a more remarkable crossover behavior is identified for the whole region II. In this case, for short scales $\alpha_1 \approx 1.5$ and for large scales $\alpha_2 \approx 0.5$.

Also, for this period and both channels, we find that these two scaling exponents are splitted by the average crossover point $\overline{n}_\times \approx 14$, which corresponds to 28 seconds, that is, approximately a half minute in time scale. We also performed the same crossover analysis to the data from Coyuca station (see Fig. 8).

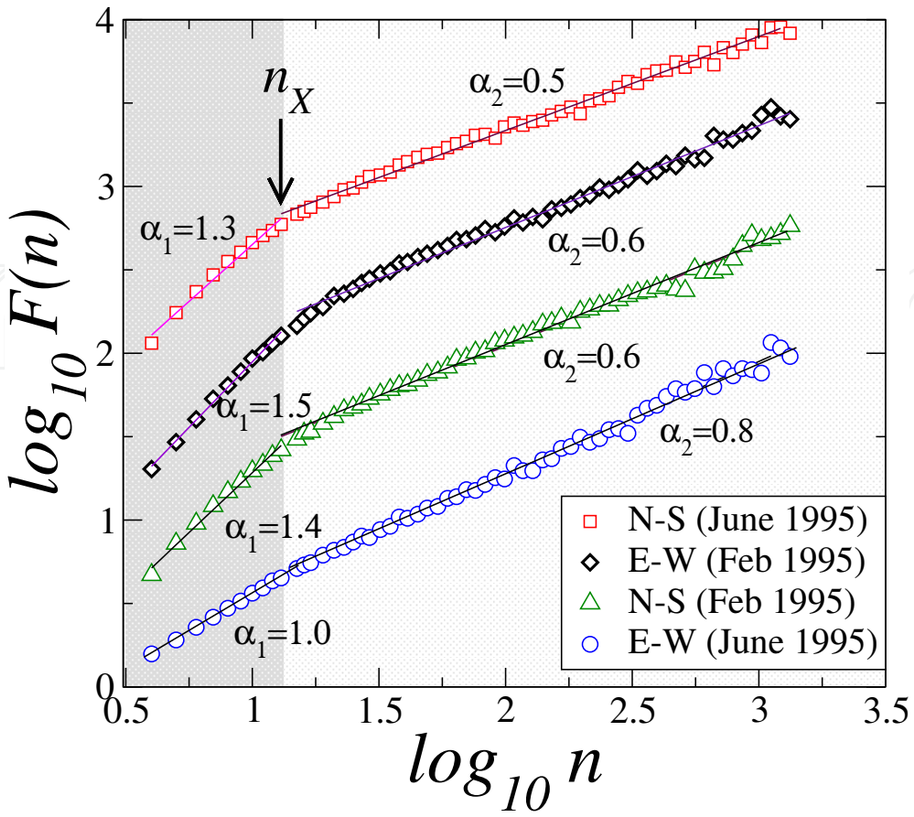


Fig. 6. Representative plots of $\log F(n)$ vs. $\log n$ for segments from Acapulco station during 1995. We observe that two scaling regimes can be defined to describe correlations. We calculated $\alpha_1$ and $\alpha_2$ according to the procedure described in the text. We find that there is an approximate typical characteristic time at which the crossover is present in these four cases. Notice that the data from June 1995 (E-W channel, open circles) show a weak croosover with both scaling exponents close to 1, indicating long-term correlations whereas data from N-S channel (open squares) lead to a clear crossover with a value close to a random walk ($\alpha_1 \approx 1.3$) for short scales and uncorrelated fluctuations ($\alpha_2 \approx 0.5$) over large scales (Guzmán-Vargas et al., 2009).

### 3.3 Cross sample entropy results

#### 3.3.1 Simulated signals

Figure 9 shows the $C_E$ profile for the simulated signals with power spectral density of the form $f^{-\beta}$, with $0 \leq \beta \leq 1$. For each value of the spectral exponent, ten independent realizations were performed and averaged to obtain the displayed results. As can be seen, $C_E$ stays well-defined for longer sequences when longer-range correlations become present in the signal (increasing $\beta$). Specifically, we observe that for values of $\beta$ close to the white noise fluctuations ($\beta = 0$), the pattern synchrony shows a high value and persists for a sequence length of around 8 samples whereas for values of $\beta$ close to one, the $C_E$ is sligthly lower than for the uncorrelated case but it persists for a larger sequence length such that for $\beta = 1$ it is around 12 samples.

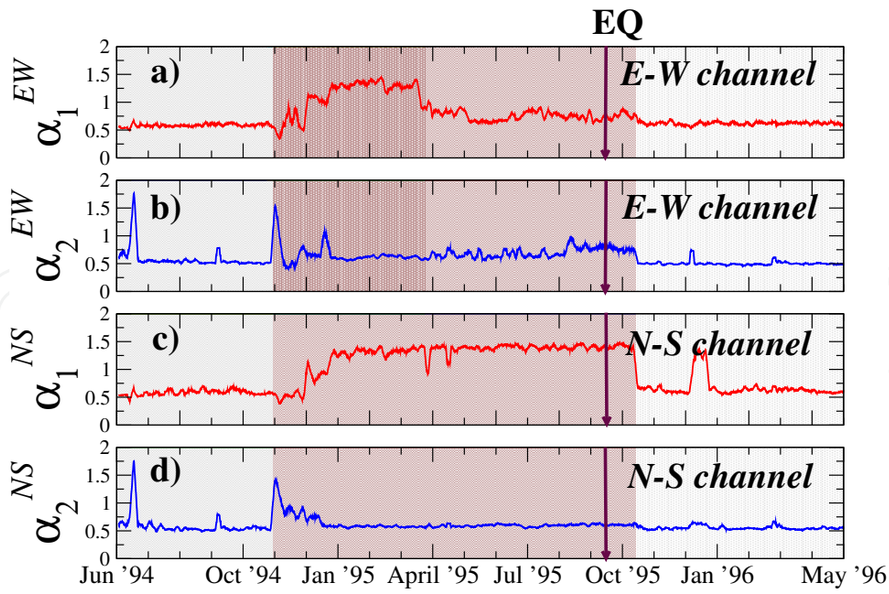


Fig. 7. Time evolution of averaged DFA-exponents for Acapulco station. The results of E-W channel are presented in Figs. 7(a) and 7(b). We also identify three main regions as in entropy results (Fig. 4(a)). For regions I and III defined in Fig. 4(a), we observe that both scaling regimes are quite similar each other with a value close to white noise behavior. In contrast, Region II display significant alterations in both scaling exponents. At the beginning of this region both exponents show an increment such that $\alpha_1$ is close to the Brownian motion value, after this period both exponents are close to one, indicating the presence of long-term correlations. For N-S channel, Regions I and III also show values close to white noise level in both short and large scales, except because the presence of a few peaks. Remarkably, Region II reveals a clear crossover with $\alpha_1^{NS} \approx 1.5$ and $\alpha_2^{NS} \approx 0.5$ (Guzmán-Vargas et al., 2009).

In addition, Figure 9 shows the results of the $C_E$ between signals with different spectral exponents $\beta_1$ and $\beta_2$, for different sequence lengths. As can be seen, the pattern synchrony between signals with correlations of longer range (for $\beta \to 1$) persists for longer sequences.

### 3.3.2 Acapulco data

The results of the $C_E$ calculation for the original and shuffled data from the Acapulco monitoring station are shown in Figure 10.

We observe regularity in the $C_E$ profile for region I. Moreover, the $C_E$ profile for the original data is not significantly different to the one obtained for the shuffled data, except that the $C_E$ reaches systematically higher values for the shuffled data. For the original data there is a period of time within June 1994 and towards the end of the region I for which the pattern synchrony remains for long sequences.

Moreover, in order to assess the effect of the data shuffling on the $C_E$ calculation, we obtain the distribution of the maximum sequence length for which the $C_E$ is well-defined (for which there is pattern synchrony), in each calculation window. In other words, for each calculation window we obtain the value of the longest data-points sequence (pattern) for which there is pattern synchrony, such that for longer sequences the value of $C_E$ is not well-defined. The

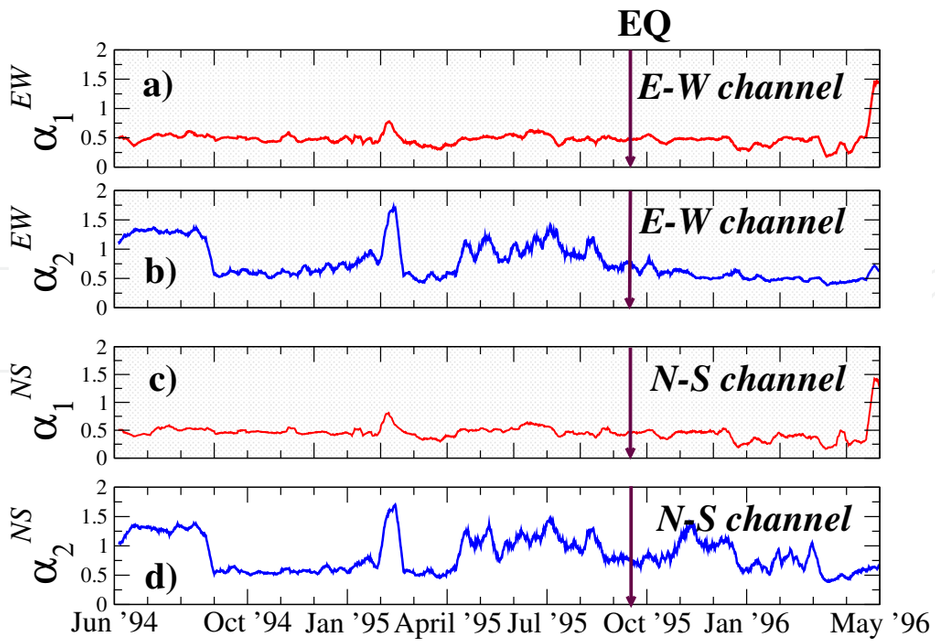


Fig. 8. Time evolution of DFA-exponents for Coyuca station. For both channels and for short scales (Figs. 8(a) and 8(c)), we observe that the exponents are close to the white noise value: $\alpha_1^{EW} = 0.52 \pm 0.26$ and $\alpha_1^{NS} = 0.49 \pm 0.20$. In contrast, for large scales the averaged exponents in both channels are bigger than 0.5 (Figs. 8(b) and 8(d)) (Guzmán-Vargas et al., 2009).

majority of the calculation windows shows presence of pattern synchrony for sequences up to 7 data-points, although for the original data we observe that there are calculation windows for which the pattern synchrony is present for longer sequences. This suggests that the pattern synchrony between the channels in this region resembles the one exhibited by white noise-like signals. This result is connected to previous works Guzmán-Vargas et al. (2008; 2009), on which we have found that for region I the signals in each channel exhibit a variability and correlations profile similar to the one for white noise.

On the other hand, we observe more variability in the $C_E$ profile for region II. In particular, notice the significant variation of the $C_E$ that occurred between January and April 1995. Also, notice that there is certain variability of the $C_E$ profile towards the end the region. From our previous studies on correlations and variability for the signals in separate channels Guzmán-Vargas et al. (2008; 2009), the geoelectrical signals for region II exhibit long-range correlations behavior; and the present results suggest that not only the channel signals individually exhibit long-range correlations, but also there is pattern synchrony between channels that persists longer than for the other regions.

#### 3.3.3 Coyuca data

The $C_E$ results for the geoelectrical signals collected by the Coyuca monitoring station are shown in Figure 11. We observe regularity in the $C_E$ profile for region I. Notice that the original data from Coyuca in region I exhibits pattern synchrony for longer sequences than for the

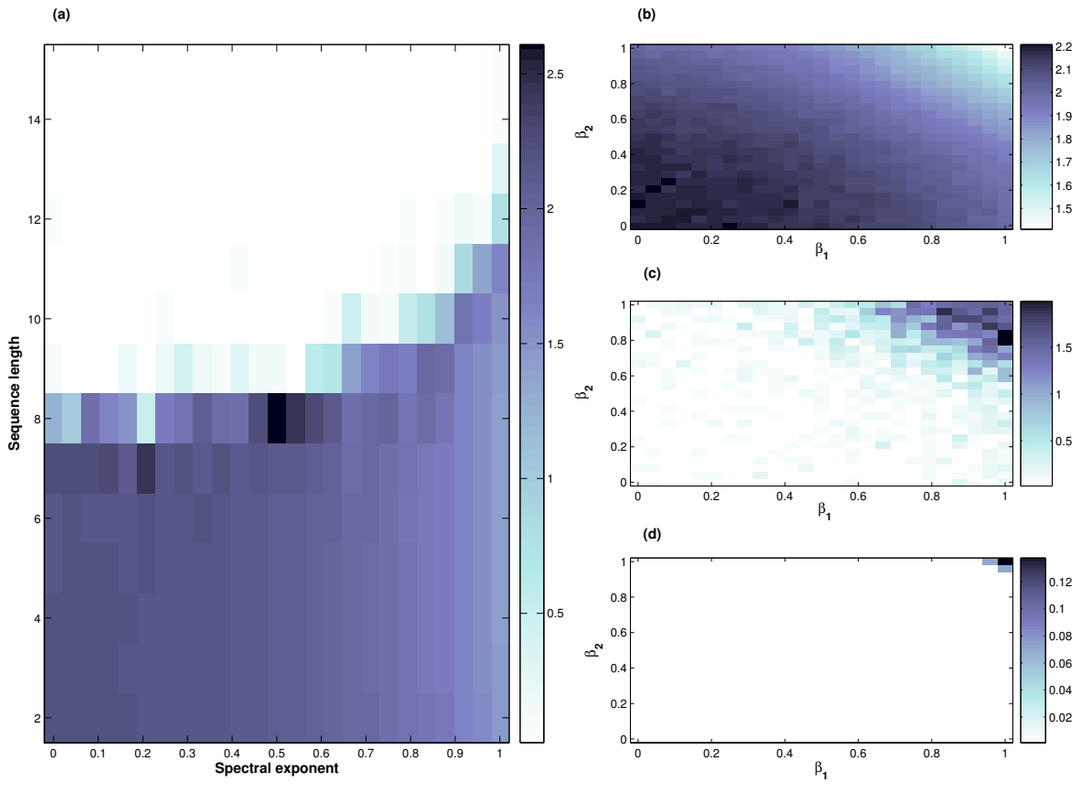


Fig. 9. Cross Sample Entropy analysis for synthetic $1/f^{\beta}$-signals, with $\beta \in [0,1]$. (a) Shows the $C_E$ between two signals with the same $\beta$; while the figures at the right show the results of $C_E$ between signals with different spectral exponents $\beta_1$ and $\beta_2$, for the sequence lengths of (b) 5, (c) 10, and (d) 15 samples (Hernández-Pérez et al., 2010).

Acapulco station, where the $C_E$ profile for the original data resembles the one obtained for the shuffled data.

On the other hand, for region II we notice the significant variation of the $C_E$ that occurs mainly between April and June 1995. Moreover, the variability of $C_E$ continues for the remaining part of the region. Comparing to the results for Acapulco station (see Figure 10), it can be seen that this signature occurred later for the Coyuca station, which was farther away from the EQ epicenter than Acapulco.

Finally, for region III we see that the $C_E$ profile at the beginning of the region shows pattern synchrony for long sequences, with some gaps towards the middle and the end of the region, on which the $C_E$ is defined for shorter sequences. Again, we observe that the $C_E$ profile for the shuffled data still shows pattern synchrony on a non-negligible number of cases for relatively long sequences, with a more even distribution. Comparing to the results from Acapulco, for the Coyuca station we observe that the effect of the shuffling reduced less the persistence of the pattern synchrony than for the Acapulco station. Again, this difference could be due to the different local properties of the crust.

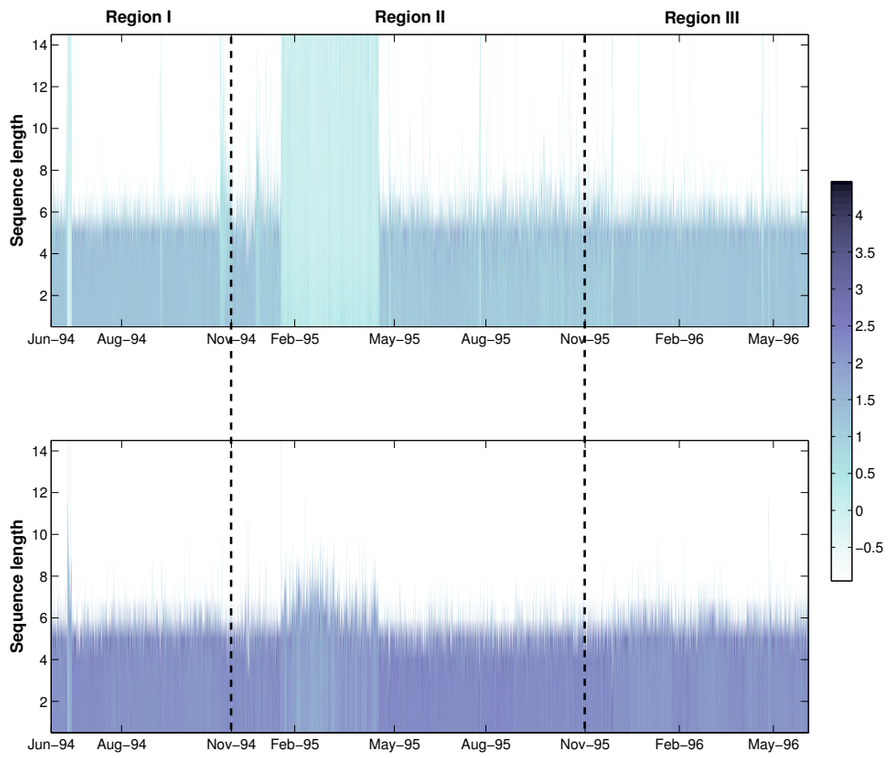


Fig. 10. Cross Sample Entropy analysis for geoelectrical time series from the Acapulco station: original (top) and shuffled data (bottom) (Hernández-Pérez et al., 2010).

### 3.4 Discussion

The $MSE$, $C_E$ and $DFA$ analyses suggest the existence of a relaxation−EQ−preparation−main shock−relaxation process along the June 1994 − May 1996 period. This process is approximately expressed for the sequence of white noise and correlated fluctuations, in the range of short and large scales. According with our findings, both scales showed important alterations along the period of observation. Remarkably, we observed correlated dynamics a few months before the main shock, especially in Acapulco station which is the nearest station to the epicenter (notice that the epicentral distance of Acapulco and Coyuca stations were 110 km and 200 km, respectively). These alterations were observed by means of MSE and DFA analyses; both methods consistently reveal that the changes in the geoelectrical potential observed prior to the main shock can be characterized by a complex and correlated behavior. In fact, MSE analysis incorporates a qualitatively visual manner to detect correlated fluctuations and it can be used as a complementary tool to characterize a complex behavior in noisy geolectric time series. From this point of view, is a very important task to identify the transition from white noise to correlated fluctuations, that is, the time at which a correlated signal is added to the white noise signal leading to the apparition of complex fluctuations and crossovers in the correlation scaling exponents. A more detailed observation of this transition

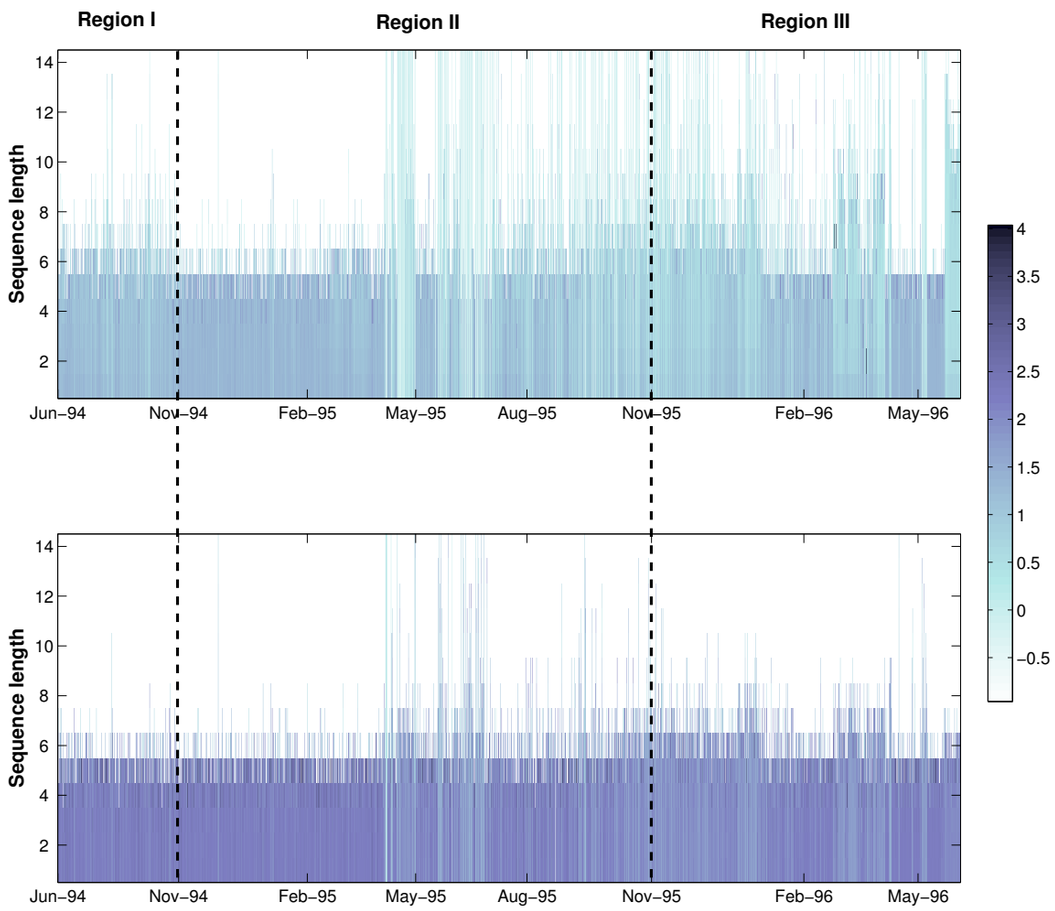


Fig. 11. Cross Sample Entropy analysis for geoelectrical time series from the Coyuca station: original (top) and shuffled data (bottom) (Hernández-Pérez et al., 2010).

located at the beginning of region II (Figs. 7a,b) reveals that, for short scales, $\alpha_1$ decreases below the white noise level ($\alpha_{WN} = 0.5$) and immediately increases displaying fluctuations in the range of correlated behavior with values close to 1.5. In contrast, for large scales, the transition occurs in the opposite direction, that is, the white noise level is altered to a value close to the Brownian motion and, after a transient period, it stabilizes around a value slightly bigger than 0.5. We have identified this transient period for E-W channel from November 1994 to March 1995 (see Fig. 4a). We remark that this transition can be understood as a sequence of erratic fluctuations ranging from anticorrelated to correlated dynamics. The fact that seemingly the precursory behavior of geolectric signal are more clear in Acapulco station agrees with the empirical threshold proposed by Hayakawa et al. (Hayakawa et al., 2007) for ultra-low-frequency (ULF) geomagnetic signals given by $0.02R \leq M - 4.5$, where $R$ is the distance between the station and the epicenter and $M$ is the EQ magnitude. We also remark

that this kind of long duration anomalies has been reported for geolectrical signals changes (lasting 56 days) for an $M = 6.6$ EQ in Japan (Uyeda et al., 2000).

## 4. Conclusions

We have explored geoelectrical signals from two sites in southern Mexico, to evaluate the changes in variability and correlations by using $MSE$, $C_E$ and $DFA$ methods. We have found different entropy values and correlation levels for these signals. In particular, the Acapulco station displays three different patterns of complex dynamics along the two year period which are clearly identified in E-W channel. This behavior can be interpreted as the geolectric expression of a relaxation-EQ preparation-mainshock-relaxation long-term process. The results for Coyuca station reveal that, for short scales, the entropy values and $DFA$ exponents are close to the white noise behavior whereas, for large scales, these quantities reflect regularity resembling a random walk. The results of both stations are qualitatively compatible with previous reports based on spectral analysis (Ramírez-Rojas et al., 2004). The conceptual difference between the Sample Entropy and, as measured by the $S_E$, and correlations, as measured by the autocorrelation function, can be expressed as follows for a time series $\{x(k)\}$. The $S_E$ deals with patterns: a sequence of data points of a certain length $m$ is taken from $\{x(k)\}$ and this pattern is searched for in whole time-series looking for matches within a tolerance $r$. However, the $S_E$ does not collect the time-stamp of the matching sequence in the time series, but counts the number of sequence matches of lengths $m$ and $m+1$. On the other hand, the objective of the autocorrelation function is to investigate the degree of dependence of future values of the time-series on present ones along the whole time series, but the time-series is not decomposed in sequences of points. Therefore, the $S_E$ analysis is complementary to the autocorrelation and spectral analysis since it operates on different features of the signals (see the *Appendix* of Ref. Pincus & Singer (1996)). Based on this, our results on the computation of the entropy and the correlation features ($DFA$) are complementary since they reveal different properties of the geoelectric signals in periods with different features as captured by each monitoring station.

In summary, $MSE$, $C_E$ and $DFA$-correlation analyses reveal important information about the complex behavior of these fluctuations and the consistent use of both methods are important complementary tools in the search of possible geoelectric precursory phenomena of earthquakes

## 5. Acknowledgments

This work was partially supported by CONACYT (project No. 49128-F-26020), COFAA-IPN, SIP-IPN and EDI-IPN.

## 6. References

Chen, Z., Ivanov, P. C., Hu, K. & Stanley, H. E. (2002). Effect of nonstationarities on detrended fluctuation analysis, *Phys. Rev. E* 65(4): 041107.

Cicerone, R. D., Ebel, J. E. & Britton, J. (2009). A systematic compilation of earthquake precursors, *Tectonophysics* 476(3-4): 371 – 396.

Costa, M., Goldberger, A. L. & Peng, C.-K. (2005). Multiscale entropy analysis of biological signals, *Phys. Rev. E* 71. 021906.

Costa, M., Goldberger, A. L. & Peng, C.-P. (2002). Multiscale entropy analysis of physiologic time series, *Phys. Rev. Lett* 89. 068102.

Eckmann, J.-P. & Ruelle, D. (1985). Ergodic theory of chaos and strange atractors, *Rev. Mod. Phys.* 57: 617.

Flores-Márquez, E. L., Márquez-Cruz, J., Ramírez-Rojas, A., Gálvez-Coyt, G. & Angulo-Brown, F. (2007). A statistical analysis of electric self-potential time series associated to two 1993 earthquakes in mexico, *Natural Hazards and Earth System Sciences* 7: 549–556.

Gershenzon, N. I., Gokhberg, M. B. & Yunga, S. L. (1993). On the electromagnetic field of an earthquake focus, *Phys. Earth Planet. Inter.* 77. 13-19.

Gotoh, K. H. Hayakawa, M., Smirnova, N. (2003). Fractal analysis of the gromagnetic data obtained at izu peninsula, japan in relation to the nearby earthquake swarm of june-august 2000, *Natural Hazards and Earth System Sciences* 3: 229–236.

Gotoh, K., Hayakawa, M., Smirnova, N. A. & K., H. (2004). Fractal analysis of seismogenic ulf emissions, *Phys. Chem. Earth* 29: 419–424.

Grassberger, P. & Procaccia, I. (1983). Estimating the kolmogorov entropy from a chaotic signal, *Phys. Rev. A* 28. 2591.

Guzmán-Vargas, L., Ramírez-Rojas, A. & Angulo-Brown, F. (2008). Multiscale entropy analysis of electroseismic time series, *Natural Hazards and Earth System Sciences* 8(4): 855–860.

Guzmán-Vargas, L., Ramírez-Rojas, A., Hernández-Pérez, R. & Angulo-Brown, F. (2009). Correlations and variability in electrical signals related to earthquake activity, *Physica A: Statistical Mechanics and its Applications* 388(19): 4218 – 4228.

Haartsen, M. W. & Pride, S. R. (1997). Electroseismic waves from point sources in layered media, *J. Geophys. Res.* 102. 24, 745-769.

Hayakawa, M. (1999). *Atmospheric and Ionospheric Phenomena Associated with Earthquakes*, Terra Sc. Publ., Tokyo.

Hayakawa, M., Hattory, K. & Ohta, K. (2007). Monitoring of ulf (ultra-low-frequency) geomagnetic variations associated with earthquakes, *Sensors* 7. 1108-1122.

Hayakawa, M. & Molchanov, O. A. (2002). *Seismo Electromagnetics: Lithosphere-Atmosphere-Ionosphere Coupling*, Terra Sc. Publ., Tokyo.

Hernández-Pérez, R., Guzmán-Vargas, L., Ramírez-Rojas, A. & Angulo-Brown, F. (2010). Pattern synchrony in electrical signals related to earthquake activity, *Physica A* 389(6): 1239 – 1252.

Honkura, Y., Isikara, A. M., Oshiman, N., Ito, A., Ucer, B., Baris, S., Tuncer, M. K., Matsushima, M., Pektas, R., Celik, C., Tank, S. B., Takahashi, F., Nakanishi, M., Yoshimura, R., Ikeda, Y. & Komut, T. (2000). Preliminary results of multidisciplinary observations before, during and after the kocaeli (izmit) earthquake in the western part of the north anatolian fault zone, *Earth Planets Space* 52. 293-298.

Ida, Y., Hayakawa, M., Adalev, A. & Gotoh, K. (2005). Multifractal analysis for the ulf geomagnetic data during the 1993 guam earthquake, *Nonlinear Processes Geophys.* 12: 157–162.

Ida, Y., Hayakawa, M. (2006). Fractal analysis for the ulf data during the 1993 guam earthquake to study prefracture criticality, *Nonlinear Processes Geophys.* 13: 409–412.

Ishido, T. & Mizutani, H. (1981). Experimental and theoretical basis of electrokinetic phenomena in rock-water systems and its application to geophysics, *J. Geophys. Res.* 86. 1763-1775.

Iyemori, T., Kamei, T., Tanaka, Y., Takeda, M., Hashimoto, T., Araki, T., Okamoto, T., Watanabe, K., Sumitomo, N. & Oshiman, N. (1996). Co-seismic geomagnetic variations observed at the 1995 hyogoken-nanbu earthquake, *J. Geomag. Geoelectr.* 48. 1059-1070.

Lazaridou, M., Varotsos, C., Alexopoulos, K. & Varotsos, P. (1985). Point defectparameters of lif, *J. Physics C: Solid State* 18: 3891–3895.

Lomnitz, C. (1990). *Fundamentals of Earthquake Prediction*, John Wiley and Sons, New York, NY.

Makse, H., Havlin, S., Schwartz, M. & Stanley, H. E. (1996). Method for generating long-range correlations for large systems, *Phys. Rev. E* 53: 5445–5449.

Matsushima, M., Honkura, Y., Oshiman, N., Baris, S., Tuncer, M. K., Tank, S. B., Celik, C., Takahashi, F., Nakanishi, M., Yoshimura, R., Pektas, R., Komut, T., Tolak, E., Ito, A., Iio, Y. & Isikara, A. M. (2002). Seimo-elecromagnetic effect associated with the izmit earthquake and its aftershocks, *Bull. Seismol. Soc. Am.* 92. 350-360.

Mizutani, H., Ishido, T., Yokokura, T. & Ohnishi, S. (1976). Electrokinetic phenomena associated with earthquakes, *Geophys. Res. Lett.* 3. 365-368.

Muñoz Diosdado, A., Pavía-Miller, C. G., Angulo-Brown, F. & Ramírez-Rojas, A. (2004). Spectral and multifractal study of electroseismic time series associated to the mw=6.5 earthquake of 24 october 1993 in mexico, *Natural Hazards and Earth System Sciences* 4. 703-709.

Peng, C. K., Havlin, S., Stanley, H. E. & Goldberger, A. L. (1995a). Long-range anti-correlations and non- gaussian behavior of the heartbeat, *Phys. Rev. Lett.* 70: 1343–1346.

Peng, C. K., Havlin, S., Stanley, H. E. & Goldberger, A. L. (1995b). Quantification of scaling exponents and crossover phenomena in nonstationary heartbeat time series, *Chaos* 5: 82–87.

Pincus, S. M. (1991). Approximate entropy as a measure of system complexity, *Proc. Natl. Acad. Sci.* 88. 2297.

Pincus, S. M. (1995). Approximate entropy (apen) as a complexity measure, *Chaos* 5: 110.

Pincus, S. & Singer, B. H. (1996). Randomness and degrees of irregularity, *Proceedings of the National Academy of Sciences* 93(5): 2083–2088.

Ramírez-Rojas, A., Flores-Márquez, E. L., Guzmán-Vargas, L., Gálvez-Coyt, G., Telesca, L. & Angulo-Brown, F. (2008). Statistical features of seismoelectric signals prior to m7.4 guerrero-oaxaca earthquake (mexico), *Natural Hazards and Earth System Sciences* 8(5): 1001–1007.

Ramírez-Rojas, A., Flores-Márquez, E. L., Guzmán-Vargas, L., Márquez-Cruz, J., Pavía-Miller, C. G. & Angulo-Brown, F. (2007). A comparison of ground geoelectric activity between three regions of different level of seismicity, *Natural Hazards and Earth System Sciences* 7: 591–598.

Ramírez-Rojas, A., Pavía-Miller, C. G. & Angulo-Brown, F. (2004). Statistical behavior of the spectral exponent and the correlation time of electric self-potential time series

associated to the ms=7.4 september 14, 1995 earthquake in mexico., *Phys. Chem. Earth.* 29: 4–9.

Richman, J. S. & Moorman, J. R. (2000). Physiological time-series analysis using approximate entropy and sample entropy, *Am. J. Physiol. Heart Circ. Physiol.* 278: H2049.

Smirnova, N., Hayakawa, M. & K., G. (2004). Precursory behavior of fractal characteristics of the ulf electromagnetic fields in seismic active zones before strong earthquakes, *Phys. Chem. Earth.* 29: 445–451.

Telesca, L. & Lapenna, V. (2006). Measuring multifractality in seismic sequences, *Tectonophysics* 423: 115–123.

Telesca, L. Lapenna, V. & M., M. (2005). Multifractal fluctuation in earthquake related geoelectrical signals, *New J. Phys.* 7: 214.

Telesca, L., Lovallo, M., Alejandro, R.-R. & Angulo-Brown, F. (2009). Scaling instability in self-potential earthquake-related signals, *Physica A: Statistical Mechanics and its Applications* 388(7): 1181 – 1186.

Uyeda, S., Nagao, T. & Kamogawa, M. (2008). Short-term earthquake prediction: Current status of seismo-electromagnetics, *Tectonophysics* . doi:10.1016/j.tecto.2008.07.019.

Uyeda, S., Nagao, T., Orihara, Y., Yamaguchi, T. & Takahashi, I. (2000). Geolectric potential changes: Possible precursors to earthquakes in japan, *Proc. Natl. Acad. Sci. U.S.A.* 97: 4561–4566.

Varotsos, P. (1980). Determination of the dielectric constant of alkali halide mixed crystals, *Physica Status Solidi B* 100: 133–138.

Varotsos, P. A. (1978). An estimate of the pressure dependence of the dielectric constant inalkali halides, *Physica Status Solidi B* 90: 339–343.

Varotsos, P. A. (2005). *The Physics of Seismic Electric Signals*, TerraPub, Tokyo.

Varotsos, P. A., Sarlis, N. V. & Skordas, E. S. (2003a). Attempt to distinguish electric signals of a dichotomous nature, *Phys. Rev. E* 68(3): 031106.

Varotsos, P. A., Sarlis, N. V. & Skordas, E. S. (2003b). Electric fields that "arrive" before the time derivative of the magnetic field prior to major earthquakes, *Phys. Rev. Lett.* 91(14): 148501.

Varotsos, P. A., Sarlis, N. V. & Skordas, E. S. (2003c). Long-range correlations in the electric signals that precede rupture: Further investigations, *Phys. Rev. E* 67(2): 021109.

Varotsos, P. A., Sarlis, N. V., Skordas, E. S. & Lazaridou, M. S. (2004). Entropy in the natural time domain, *Phys. Rev. E* 70(1): 011106.

Varotsos, P. A., Sarlis, N. V., Skordas, E. S. & Lazaridou, M. S. (2008). Fluctuations, under time reversal, of the natural time and the entropy distinguish similar looking electric signals of different dynamics, *J. Appl. Phys.* 103. 014906.

Varotsos, P. A., Sarlis, N. V., Tananaka, H. K. & Skordas, E. S. (2005). Some properties of the entropy in the natural time, *Phys. Rev. E* 71(1): 032102.

Varotsos, P. & Alexopoulos, K. (1984a). Physical properties of the variations of the electric field of the earth preceding earthquakes i, *Tectonophysics* 110. 73-98.

Varotsos, P. & Alexopoulos, K. (1984b). Physical properties of the variations of the electric field of the earth preceding earthquakes ii. determination of epicenter and magnitude, *Tectonophysics* 110: 99âĂŞ125.

Varotsos, P. & Alexopoulos, K. (1986). *Stimulated current emission in the earth and related geophysical aspects. In: Amelinckx, S., Gevers, R., Nihoul, J. (Eds.), Thermodynamics on Point Defects and their Relation with Bulk Propierties*, North Holland, Amsterdam.

Veldhuis, J. D., Iranmanesh, A., Mulligan, T. & Pincus, S. M. (1999). Disruption of the young-adult synchrony between luteinizing hormone release and oscillations in follicle-stimulating hormone, prolactin, and nocturnal penile tumescence (npt) in healthy older men, *Journal of Clinical Endocrinology and Metabolism* 84(10): 3498–3505.

Yépez, E., Angulo-Brown, F., Peralta, J. A., Pavía-Miller, C. G. & González-Santos, G. (1995). Electric fields patterns as seismic precursors, *Geophys. Res. Lett.* 22: 3087–3090.

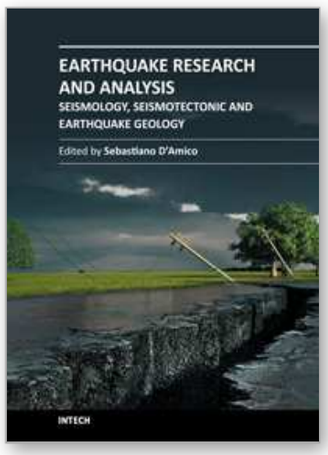


**Earthquake Research and Analysis - Seismology, Seismotectonic and Earthquake Geology**

Edited by Dr Sebastiano D'Amico

ISBN 978-953-307-991-2
Hard cover, 370 pages
**Publisher** InTech
**Published online** 08, February, 2012
**Published in print edition** February, 2012

This book is devoted to different aspects of earthquake research. Depending on their magnitude and the placement of the hypocenter, earthquakes have the potential to be very destructive. Given that they can cause significant losses and deaths, it is really important to understand the process and the physics of this phenomenon. This book does not focus on a unique problem in earthquake processes, but spans studies on historical earthquakes and seismology in different tectonic environments, to more applied studies on earthquake geology.

**How to reference**

In order to correctly reference this scholarly work, feel free to copy and paste the following:

L. Guzmán-Vargas, R. Hernández-Pérez, F. Angulo-Brown and A. Ramírez-Rojas (2012). Some Complexity Studies of Electroseismic Signals from Mexican Subduction Zone, Earthquake Research and Analysis - Seismology, Seismotectonic and Earthquake Geology, Dr Sebastiano D'Amico (Ed.), ISBN: 978-953-307-991-2, InTech, Available from: http://www.intechopen.com/books/earthquake-research-and-analysis-seismology-seismotectonic-and-earthquake-geology/some-complexity-studies-of-electroseismic-signals-from-the-mexican-subduction-zone

INTECH
open science | open minds

**InTech Europe**
University Campus STeP Ri
Slavka Krautzeka 83/A
51000 Rijeka, Croatia
Phone: +385 (51) 770 447
Fax: +385 (51) 686 166
www.intechopen.com

**InTech China**
Unit 405, Office Block, Hotel Equatorial Shanghai
No.65, Yan An Road (West), Shanghai, 200040, China
中国上海市延安西路65号上海国际贵都大饭店办公楼405单元
Phone: +86-21-62489820
Fax: +86-21-62489821

IntechOpen